COHERENT SINGLE PION PRODUCTION BY ANTINEUTRINO CHARGED CURRENT INTERACTIONS AND TEST OF PCAC.

BEBC WA59 Collaboration

P. Marage[3,*], M. Aderholz[9], P. Allport[10], N. Armenise[1], J.P. Baton[12], M. Berggren[13], D. Bertrand[3,**], V. Brisson[6], F.W. Bullock[14], W. Burkor[8], M. Calicchio[1], E.F. Clayton[7], T. Coghen[8], A.M. Cooper-Sarkar[11], O. Erriquez[1], P.J. Fitch[14], G. Gerbier[12], J. Guy[11], F. Hamisi[7], P.O. Hulth[13], G.T. Jones[2], P. Kasper[11,***], H. Klein[4], R.P. Middleton[2,+,++], D.B. Miller[7], M.M. Mobayyen[7], D.R.O. Morrison[4], S. Natali[1], M. Neveu[12], S.W. O'Neale[2], M.A. Parker[4], P. Petiau[6], J. Sacton[3], R.A. Sansum[14,+], E. Simopoulou[5], C. Vallée[6], K. Varvell[2], A. Vayaki[5], W. Venus[11], H. Wachsmuth[4], J. Wells[10,+++], W. Wittek[9].

Submitted to Zeit. fur Phys.

1 Dipartimento di Fisica dell'Universita e Sezione INFN, Bari, Italy
2 University of Birmingham, UK
3 Inter-University Institute for High Energies, ULB-VUB, Brussels, Belgium
4 CERN, Geneva, Switzerland
5 Nuclear Research Centre Demokritos, Athens, Greece
6 LPNHE, Ecole Polytechnique, Palaiseau, France
7 Imperial College of Science and Technology, London, UK
8 Institute of Nuclear Physics, Cracow, Poland
9 Max-Planck-Institut fur Physik und Astrophysik, München, Germany
10 Department of Nuclear Physics, Oxford, UK
11 Rutherford Appleton Laboratory, Chilton, Didcot, UK
12 DPhPE, Centre d'Etudes Nucléaires, Saclay, France
13 Institute of Physics, University of Stockholm, Sweden
14 Department of Physics and Astronomy, University College London, UK

* Chercheur sur ARC no 65/84-89, Belgium
** Chercheur qualifié FNRS, Belgium
*** Now at Saclay
\+ Supported by an SERC Research Studentship, UK
++ Now at Rutherford Appleton Laboratory
+++ Now at University of Glasgow, UK.

Abstract.

The cross section for coherent production of a single π^- meson in charged current antineutrino interactions on neon nuclei has been measured in BEBC to be $(175 \pm 25)\ 10^{-40}\ cm^2$/neon nucleus, averaged over the energy spectrum of the antineutrino wide band beam at the CERN SPS; this corresponds to $(0.9 \pm 0.1)\%$ of the total charged current $\bar{\nu}_\mu$ cross section. The distributions of kinematical variables are in agreement with theoretical predictions based on the PCAC hypothesis and the meson dominance model; in particular, the Q^2 dependence is well described by a propagator containing a mass $m = (1.35 \pm 0.18)$ GeV. The absolute value of the cross section is also in agreement with the model. This analysis thus provides a test of the PCAC hypothesis in the antineutrino energy range 5-150 GeV.

1. INTRODUCTION.

Evidence for coherent charged current interactions of antineutrinos on neon nuclei has been reported in a previous publication[1]. The data came from an exposure of the bubble chamber BEBC, filled with a 75 mole % Ne/H_2 mixture, to the antineutrino wide band beam at the CERN SPS. Charged current antineutrino interactions with positive muons of momentum greater than 5 GeV were selected with the external muon identifier (EMI). The total number of coherent events with one negatively charged hadron, with or without associated gammas, was found to be (234 $\pm$ 26) events, which corresponds to (1.4 $\pm$ 0.1)% of the total antineutrino cross section for charged current interactions with $p_{\mu^+} > 5$ GeV.

In this paper, the exclusive channel

$$\bar{\nu}_\mu + Ne \rightarrow \mu^+ + \pi^- + Ne \qquad (1)$$

which dominates the coherent interaction cross section, is analyzed. The study of the differential distributions is an important feature of this experiment : it allows one to test the predictions of a model based on the Partial Conservation of the Axial Current (PCAC) hypothesis and the meson dominance model, and in particular the parameterization of the Q^2 distribution. The comparison of the predicted and measured absolute cross sections provides a test of the PCAC hypothesis in the SPS energy range.

Coherent π° meson production in ν and $\bar{\nu}$ neutral current interactions has been observed at the CERN PS[2], although with less statistical significance. The CHARM collaboration[3] has observed the same neutral current reactions at the SPS with statistical errors comparable to ours but with higher systematic uncertainties due to corrections for background and cuts. Finally, a signal for coherent pion production in charged current as well as neutral current interactions has been observed in the SKAT bubble chamber at Serpukhov[4].

2. THE COHERENT SIGNAL.

In coherent interactions, the nucleus recoils as a whole, without breakup; it acquires low recoil momentum and therefore remains undetected in the bubble chamber. Coherent interactions are characterized by an exponentially falling $|t|$ distribution, where t is the square of the 4-momentum transfer to the nucleus :

$$\frac{d\sigma}{dt} \sim e^{-b|t|}, \qquad (2)$$

$b^{1/2}$ being of the order of the transverse dimensions of the nucleus.

Fig. 1 shows the experimental distributions of $|t|$ for events with a μ^+ and only a π^- meson (no associated gammas) in the final state, with and without stubs; a stub is defined as a nuclear fragment or a proton with momentum less than 300 MeV, and signals nuclear breakup. The coherent signal is the peak at $|t| < 0.1$ GeV^2 for the events without stub. The background under this peak coming from incoherent interactions is obtained from the $|t|$-distribution of the events with stubs; this procedure avoids systematic uncertainties in the background extrapolation [1].

For $|t| < 0.1$ GeV^2 and $p_{\mu^+} > 5$ GeV, the coherent production of a single π^- (without gamma) amounts to (155 ± 20) events, i.e. (66 ± 4)% of all coherent events with one negatively charged hadron (with or without gammas), or (0.9 ± 0.1)% of the total antineutrino charged current cross section averaged over the energy spectrum of the SPS wide band beam.

In computing the total cross section for reaction (1), the following corrections have been taken into account :

(i) Events with the hadron interacting too close to the vertex to measure its charge were discarded, and the remaining events were weighted according to the hadron energy; this average weight was 1.075;

(ii) Two different double scans were performed on all the film, and the combined efficiency for two-prong events without gammas was found to be (90 ± 3)%;

(iii) A Monte Carlo simulation, which will be presented below, indicates that about 2.5 % of the coherent $\mu^+\pi^-$ events have measured $|t|$ values greater than the cut at 0.1 GeV^2;

(iv) According to the Monte Carlo simulation, the minimum momentum of 5 GeV required for muon identification in the EMI leads to an average loss of 3.5 % of the events, ranging from about 10 % for $E_{\bar{\nu}}$ between 5 and 20 GeV, down to less than 1 % for $E_{\bar{\nu}}$ above 30 GeV;

(v) Coherent ρ^- and A_1^- production can contribute to the $\mu^+ \pi^-$ signal if all the gammas from π° meson decays ($\rho^- \to \pi^- \pi^\circ$; $A_1^- \to \rho^- \pi^\circ$) escape detection; estimates of coherent ρ^- and A_1^- production and of the gamma detection efficiency for two-prong events lead to a contribution of (2 ± 1) events;

(vi) Coherent π^- production can lead to $\mu^+ \pi^- \gamma$ events in case of muon inner bremsstrahlung; this loss is estimated to be (3 ± 3) events by comparing the $|t|$ distributions of $\mu^+ \pi^- \gamma$ events with $\cos\theta(\mu,\gamma) > 0.995$, with and without stubs.

The corrected total number of events due to coherent single π^- production is thus (166 ± 22) events. This corresponds to an absolute cross section of $(175 \pm 25) \times 10^{-40}$ cm^2/neon nucleus, averaged over the $\bar{\nu}_\mu$ energy spectrum, which extends from 5 to 200 GeV, with a mean energy of 27 GeV. This cross section is obtained from the total number of charged-current events, assuming $\sigma/E = (0.35 \pm 0.02) \times 10^{-38}$ cm^2 GeV^{-1} per nucleon for the $\bar{\nu}_\mu$ charged current cross section(5), and correcting for the 4 % of interactions on the hydrogen in the Ne/H_2 mixture.

3. THEORETICAL PREDICTIONS.

As discussed by several authors(6-8), reaction (1) can be described by the diagrams displayed in Fig. 2; graphs 2a and 2b represent the contribution of the axial-vector component of the weak current, and graph 2c the contribution of the vector component.

Let us discuss these various contributions separately :

a) In the limit of vanishing final state lepton mass ($m_l = 0$), the contribution of the axial-vector component reduces to diagram 2a. It is evaluated by using Adler's theorem(6,7) according to which, at $Q^2 = 0$ (Q^2 is the square of the 4-momentum transfer from the leptons to the hadrons), the matrix element for the reaction

$$\nu + \alpha \to l + \beta \qquad (\alpha \neq \beta) \tag{3}$$

is proportional to the divergence of the axial-vector current $\partial_\mu A^\mu$. The PCAC hypothesis states that $\partial_\mu A^\mu = f_\pi \phi_\pi$, where f_π is the pion decay constant and ϕ_π is the pion field. Hence the axial-vector weak current at $Q^2 = 0$ behaves like a pion and the cross section for reaction (3) is proportional to that for the reaction

$$\pi + \alpha \rightarrow \beta \quad , \tag{4}$$

the strength of the process being fixed by f_π. This implies that the cross section for reaction (1) at $Q^2 = 0$ is proportional to the elastic pion-nucleus cross section. Due to angular momentum conservation at $Q^2 = 0$, only the longitudinal component of the weak axial-vector current (A_L^-) couples to the final state π^-. In the framework of the meson dominance model, this process corresponds to the diffractive scattering off the nucleus of $J^{PC} = 1^{++}$ states, dominated by the A_1 resonance; it is diffractive scattering because the $\rho°$ exchange is forbidden by isospin conservation. The Q^2 dependence of this contribution is thus described by a propagator of the form $\left(\frac{m_A^2}{m_A^2+Q^2}\right)^2$, where m_A is the axial-vector meson mass.

b) As the axial-vector current is not conserved, it has also a component proportional to the gradient of the pion field (graph 2b), which gives rise to a term proportional to the lepton mass squared (m_l^2) in the cross section. It turns out that this contribution accounts for only 0.2 % of the total cross section in the present experiment.

c) In general, there is also a vector current contribution to the cross section. At $Q^2 = 0$, this contribution vanishes because of the conservation of the vector current (CVC). At $Q^2 \neq 0$, it is negligible in the case of coherent production of a single pion on an isoscalar target : the vector current behaves like a ρ meson which would convert to a π meson by exchange of an isoscalar ω-like object (graph 2c). This exchange is kinematically suppressed in the forward direction, which is the t range favoured in the coherent reaction.

The cross section for reaction (1) is (see[7,8]) :

$$\frac{d^3\sigma}{dQ^2 d\nu dt} = \frac{G^2}{2\pi^2} f_\pi^2 \frac{d\sigma(\pi Ne \to \pi Ne)}{dt}$$

$$\times \frac{1}{\nu} \left[\frac{P_\mu}{E_{\bar\nu}} \left(\frac{m_A^2}{m_A^2+Q^2}\right)^2 - \frac{\nu}{E_{\bar\nu}} \frac{m_A^2}{m_A^2+Q^2} \frac{m_1^2}{m_\pi^2+Q^2} + \frac{1}{4} \frac{\nu^2}{E_{\bar\nu}^2} \frac{m_1^2 (m_1^2+Q^2)}{(m_\pi^2+Q^2)^2} \right], \quad (5)$$

where $G = 1.166 \times 10^{-5}$ GeV^{-2} is the weak coupling constant, $f_\pi = 0.93\ m_\pi$ and $\nu = E_{\bar\nu} - E_{\mu^+} \simeq E_{\pi^-}$. The first term in this expression corresponds to graph 2a, the last term corresponds to graph 2b, and the middle term arises from the interference of the two graphs.

Rein and Sehgal[8] describe the π-Ne elastic cross section in the following way :

$$\frac{d\sigma(\pi Ne \to \pi Ne)}{dt} = \frac{A^2}{16\pi} \sigma_{tot}^2(\pi\text{-}N)(1+r^2)\, e^{-b|t|}\, F_{abs}, \quad (6)$$

where $A = 20$ is the neon atomic number, σ_{tot} (π-N) is the total pion-nucleon cross section at $E_\pi = \nu$, $r^2 = \left|\frac{\mathrm{Re}\, f_{\pi N}(0)}{\mathrm{Im}\, f_{\pi N}(0)}\right|^2$ is taken to be 0, and $b = 1/3\, R^2$ (R is the effective nuclear radius). The factor F_{abs}, which accounts for the reinteractions of the pion inside the nucleus, is expressed by a simple model as

$$F_{abs} = e^{-\langle x\rangle/\lambda}, \quad \lambda^{-1} = \sigma_{inel}^{\pi\text{-}N}\, \rho, \quad (7)$$

where $\langle x\rangle$ is the average path length of the pion in the nucleus and ρ is the nuclear density : $\rho = A\left(\frac{4\pi}{3} R^3\right)^{-1}$.

4. COMPARISON OF THE COHERENT SIGNAL WITH THEORETICAL PREDICTIONS.

a. Differential distributions.

An essential feature of a bubble chamber experiment is that it gives access to the kinematical variable distributions;

this allows one to test the predicted form of the differential cross section, and especially to determine the value of the mass m_A in the propagator of the two first terms in eq. (5).

These differential distributions are shown in Fig. 3 and 4. Within the range $|t| < 0.05$ GeV^2, there are 130 events without stubs, of which $(90 \pm 4)\%$ are estimated to be coherent, and there are 6 incoherent events with stubs. The incoherent background is obtained from the events with stubs and is subtracted from the distributions (the subtracted events are shown hatched on the figures). The experimental distributions are compared with the predictions of a Monte Carlo simulation based on eq.(5), taking into account the measurement errors and the uncertainty in the neutrino direction.

The $|t|$ distribution (Fig. 3a) shows a dip at low $|t|$-values, due to the lower kinematic limit of $|t|$: $t_{min} \simeq \left(\frac{Q^2+m_\pi^2}{2\nu}\right)^2$;

this threshold effect is eliminated by the use of the variable $t' = |t| - t_{min}$ (Fig. 3b). Table Ia shows that the mean values of $|t|$ and t' are insensitive to the value of m_A. Thus the widths of the $|t|$ and t' distributions reflect the transverse dimensions of the nucleus, broadened by the measurement errors. The curves on Fig. 3 correspond to a radius R = 3.04 fm for the neon nucleus, as measured by electron scattering[9], implying $b = 79$ GeV^{-2}. They are in good agreement with the experimental distributions. As a cross check, the value we extract from the data using the model of Rein and Sehgal is

$$R = (2.8 \pm 0.3) \text{ fm}, \qquad (8)$$

in agreement with the measured value of 3.0 fm. This confirms that the signal is due to coherent scattering on neon nuclei.

In Fig. 4, the variables $E_{\bar\nu}$, ν, Q^2, $W = (2M_p\nu - Q^2 + M_p^2)^{1/2}$, $x = Q^2/2M_p\nu$ and $y = \nu/E_{\bar\nu}$ (M_p is the proton mass) are displayed for the coherent $\mu^+\pi^-$ events with the selection

$|t| < 0.05$ GeV^2(*). In these figures, 2 events without stub with $x > 0.3$ and 2 events with $Q^2 > 4$ GeV^2 were discarded : they are attributed to incoherent background since, according to the Monte Carlo simulation, there should be no coherent event with $x > 0.3$ and only 0.3 % of the coherent events should have $Q^2 > 4$ GeV^2 (for $m_A = m_{A_1}$); 2 events with stubs are excluded by the same cuts. In Fig. 4, these distributions are compared to those for the complete sample of charged current interactions.

The mean values for $E_{\bar{\nu}}$, ν, Q^2, W, x and y are shown in table Ia, and compared with those predicted by the model for various values of m_A; it was tested that the predicted mean values are quite insensitive to variations of order 10 % in R. In table Ib, the mean values of the same variables are presented separately for $E_{\bar{\nu}} < 25$ GeV and for $E_{\bar{\nu}} > 25$ GeV.

Fig. 4c shows that the Q^2-values of the coherent events are lower than those for other charged current events (for which $\langle Q^2 \rangle = 4.2$ GeV^2), but do extend up to 2 GeV^2. The insert in the Fig. shows that the data are described by the model also at the smallest Q^2-values. As the Q^2 variable is directly associated to the mass m_A in the propagator of the first terms of eq. (5), we use $\langle Q^2 \rangle$ to extract the value of m_A which describes our data best. We find

$$m_A = (1.35 \pm 0.18) \text{ GeV}, \qquad (9)$$

a value close to the A_1 meson mass.

The coherent events are seen on Fig. 4e to be restricted to small x-values. Furthermore, the mean x-values are similar for events at low and high $E_{\bar{\nu}}$-values (Table Ib). This behaviour is as expected for interactions with large impact parameters.

(*) W and x are calculated as in the case of scattering off a nucleon at rest, for the sake of comparison with incoherent charged current interactions. With this definition, the x-values can extend up to 20 for reaction (1); the proper definition in the case of coherent scattering on neon would be obtained by replacing the proton mass M_p by the neon mass.

b. Absolute value of the cross section.

A further test of the model is provided by the absolute value of the cross section. Indeed, the PCAC hypothesis, on which eq. (5) is based, states that the cross section for reaction (1) at $Q^2 = 0$ is proportional to the elastic pion-nucleus cross section, the proportionality factor being the pion decay constant f_π.

The experimental cross section for reaction (1) as a function of the $\bar{\nu}$ energy is presented in Fig. 5. The solid curve represents the cross section prediction when m_A is set to the A_1 mass (1.275 GeV); in this case, the absorption factor is $\langle F_{abs} \rangle = 0.43$, when averaged over the pion energy spectrum. Also shown in Fig. 5 are the predictions for $m_A = 1.15$ GeV and $m_A = 1.55$ GeV, corresponding to values of m_A about 1 standard deviation away from our estimate (9); this changes the cross sections averaged over the energy spectrum by -7 % and +9 % respectively. The sensitivity of the predicted cross section to the nuclear model has been estimated by changing R from 3.0 fm to 2.7 fm : this would increase the cross section by only $\sim$ 10 %, since the slower fall off of the $|t|$-distribution is partly compensated by the higher absorption in the more compact nucleus.

In accordance with the results presented on Fig. 5, the experimental number of coherent events is in good agreement with the number expected from the $\bar{\nu}$ energy spectrum : (166 $\pm$ 22) events are observed, whereas (147 $\pm$ 17) events are predicted for $m_A = 1.35$ GeV. The error on the predicted number accounts for the uncertainties in the values of m_A, in the $\bar{\nu}$ charged current cross section and in the shape of the $\bar{\nu}$ flux. The additional error arising from the uncertainty on the nuclear model used, is not included.

5. CONCLUSIONS.

We have studied one specific channel for the antineutrino longitudinal cross section, the coherent production of a single π^- meson on a neon nucleus by charged current interactions : $\bar{\nu}_\mu + Ne \rightarrow \mu^+ + \pi^- + Ne$. This process accounts for (0.9 $\pm$ 0.1)% of the total $\bar{\nu}_\mu$ charged current cross section, which corresponds to = (175 $\pm$ 25) 10^{-40} cm^2/neon nucleus, averaged over the energy spectrum of the $\bar{\nu}_\mu$ wide band beam at the SPS.

The differential distributions for $E_{\bar{\nu}}$, ν , Q^2, W, x, y, t and t' are in excellent agreement with the predictions of a model based on the PCAC hypothesis and the meson dominance model. The Q^2 dependence of the signal is well described by a propagator of the form $\left(\frac{m_A^2}{m_A^2 + Q^2}\right)^2$, with $m_A = (1.35 \pm 0.18)$ GeV, a value close to the A_1 meson mass.

The predictions of the model concerning the total number of coherent $\mu^+ \pi^-$ events and the energy dependence of the absolute cross section are also in good agreement with the data. This tests the basic assumption of the model which relates, through the PCAC hypothesis, the cross section for reaction (1) to the elastic pion-neon cross section, the strength of the process being given by the pion decay constant f_π.

This analysis provides thus a detailed test of the PCAC hypothesis in the antineutrino energy range 5-150 GeV.

Acknowledgements.

We express our gratitude to the CERN staff for an excellent run, and to the scanning and measuring staff in our institutions for their dedicated work. One of us (P.M.) is pleased to acknowledge enlightening discussions with J. Pestieau.

REFERENCES.

(1) a. P. MARAGE et al., Phys. Lett. 140B (1984), 137
b. W. WITTEK, Proceedings of the XIth International Conference on Neutrino Physics and Astrophysics, Dortmund 1984, p. 458.

(2) a. H. FAISSNER et al., Phys. Lett. 125B (1983), 230
b. E. ISIKSAL, D. REIN and J.G. MORFIN, Phys. Rev. Lett. 52 (1984), 1096.

(3) F. BERGSMA et al., Phys. Lett. 157B (1985), 469.

(4) H.J. GRABOSCH et al., Coherent pion production in neutrino and antineutrino interactions on nuclei of heavy freon molecules, PHE 85-12 (1985).

(5) M. ADERHOLZ et al., WA21-WA59 Collaborations, submitted to Phys. Lett. B

(6) S.L. ADLER, Phys. Rev. 135B (1964), 963.

(7) C.A. PIKETTY and L. STODOLSKY, Nucl. Phys. B15 (1970), 571.

(8) D. REIN and L.M. SEHGAL, Nucl. Phys. B223 (1983), 29.

(9) C.W. DE JAGER, H. DE VRIES and C. DE VRIES, Atomic data and Nuclear data Tables 14 (1974), 479.

FIGURE CAPTIONS.

Fig. 1 Distribution of the square of the 4-momentum transfer t, for 581 $\mu^+ \pi^-$ events without stub and for 205 events with stubs, normalised to the former for $|t| > 0.1$ GeV^2.

Fig. 2 Coherent single π^- meson production by charged current antineutrino interactions : a) diffractive scattering of the longitudinal component of the weak axial-vector current; b) diffractive scattering of a pion directly coupling to the weak axial-vector current; c) scattering of the weak vector current, via ω-exchange.

Fig. 3 Distributions a) for $|t|$, the square of the 4-momentum transfer to the nucleus; b) for $t' = |t| - t_{min}$, for the $\mu^+ \pi^-$ coherent events with $|t| < 0.05$ GeV^2 (the incoherent background, estimated from the events with stubs, is shown hatched). The curves, normalised to the coherent signal, are predictions of the model with $m_A = m_{A_1}$ and b = 79 GeV^{-2}, including the effects of experimental resolution.

Fig. 4 Distributions of a) $E_{\bar{\nu}}$; b) $\nu = E_{\bar{\nu}} - E_{\mu^+}$; c) Q^2; d) $W = (2M_p \nu - Q^2 + M_p^2)^{1/2}$; e) $x = Q^2/2M_p\nu$; f) $y = \nu/E_{\bar{\nu}}$ for the $\mu^+ \pi^-$ coherent events with $x < 0.3$, $Q^2 < 4$ GeV^2 and $|t| < 0.05$ GeV^2 (the incoherent background, estimated from the events with stubs, is shown hatched). The solid curves, normalised to the coherent signal, correspond to the predictions of the model with $m_A = m_{A_1}$, including the effects of experimental resolution. The dashed histograms represent the distributions for the complete sample of charged current interactions, divided by a factor 100.

Fig. 5 Cross section for coherent single π^- meson production by charged current antineutrino interactions on neon nuclei as a function of the $\bar{\nu}$ energy $E_{\bar{\nu}}$; the curves are predictions of the model. Data for pion coherent production in other experiments(2,4) have been scaled to correspond to charged current interactions on neon nuclei; the lower (higher) energy point for the CHARM experiment(3) corresponds to $\bar{\nu}_\mu(\nu_\mu)$ interactions.

	Data		Model		
			m_A=1.15 GeV	m_A=1.275 GeV (= m_{A_1})	m_A=1.55 GeV
$\langle E_{\bar{\nu}} \rangle$ (GeV)	30.4	± 2.0	29.3	29.6	29.8
$\langle \nu \rangle$ (GeV)	4.8	± 0.4	4.4	4.7	5.1
$\langle Q^2 \rangle$ (GeV^2)	0.375	± 0.04	0.325	0.355	0.415
$\langle W \rangle$ (GeV)	2.76	± 0.11	2.62	2.68	2.80
$\langle x \rangle$	0.058	± 0.004	0.057	0.057	0.059
$\langle y \rangle$	0.184	± 0.014	0.160	0.167	0.181
$\langle \|t\| \rangle$ (GeV^2)	0.0196	± 0.0012	0.0184	0.0184	0.0187
$\langle t' \rangle$ (GeV^2)	0.0149	± 0.0011	0.0138	0.0139	0.0140

Table Ib.

	$E_{\bar{\nu}}$ < 25 GeV			$E_{\bar{\nu}}$ > 25 GeV		
	Data		Model m_A=1.275GeV	Data		Model m_A=1.275GeV
$\langle E_{\bar{\nu}} \rangle$ (GeV)	15.7	± 0.6	17.3	46.5	± 3.0	43.1
$\langle \nu \rangle$ (GeV)	3.4	± 0.4	3.2	6.3	± 0.8	6.4
$\langle Q^2 \rangle$ (GeV^2)	0.30	± 0.03	0.28	0.46	± 0.07	0.43
$\langle W \rangle$ (GeV)	2.45	± 0.12	2.33	3.10	± 0.19	3.07
$\langle x \rangle$	0.060	± 0.005	0.061	0.056	± 0.006	0.054
$\langle y \rangle$	0.205	± 0.018	0.180	0.161	± 0.021	0.153
$\langle \|t\| \rangle$ (GeV^2)	0.0196	± 0.0016	0.0177	0.0196	± 0.0017	0.0192
$\langle t' \rangle$ (GeV^2)	0.0152	± 0.0016	0.0128	0.0145	± 0.0016	0.0151

Table I : Mean values of kinematical variables for the coherent $\mu^+ \pi^-$ events, after background subtraction for $P_\mu > 5$ GeV, $x < 0.3$, $Q^2 < 4$ GeV^2 and $|t| < 0.05$ GeV^2, compared with the model predictions for coherent single π^- meson production, using several values of m_A : a. all events; b. separately for low and high $E_{\bar{\nu}}$-values.

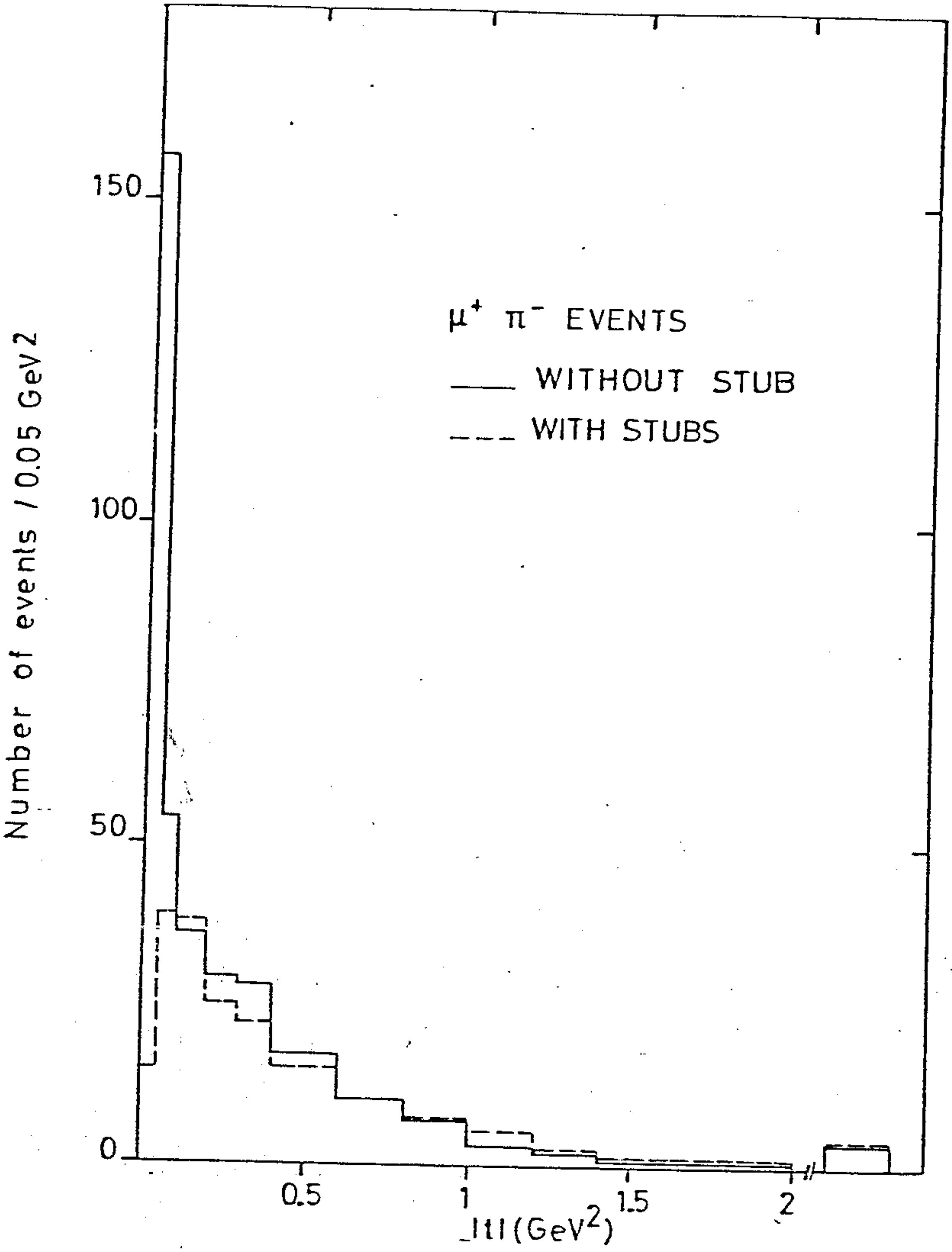

Number of events / 0.05 GeV2
150
100
50
0
0.5
1
1.5
2
|t| (GeV^2)
μ$^+$ π$^-$ EVENTS
WITHOUT STUB
WITH STUBS

Fig. 1

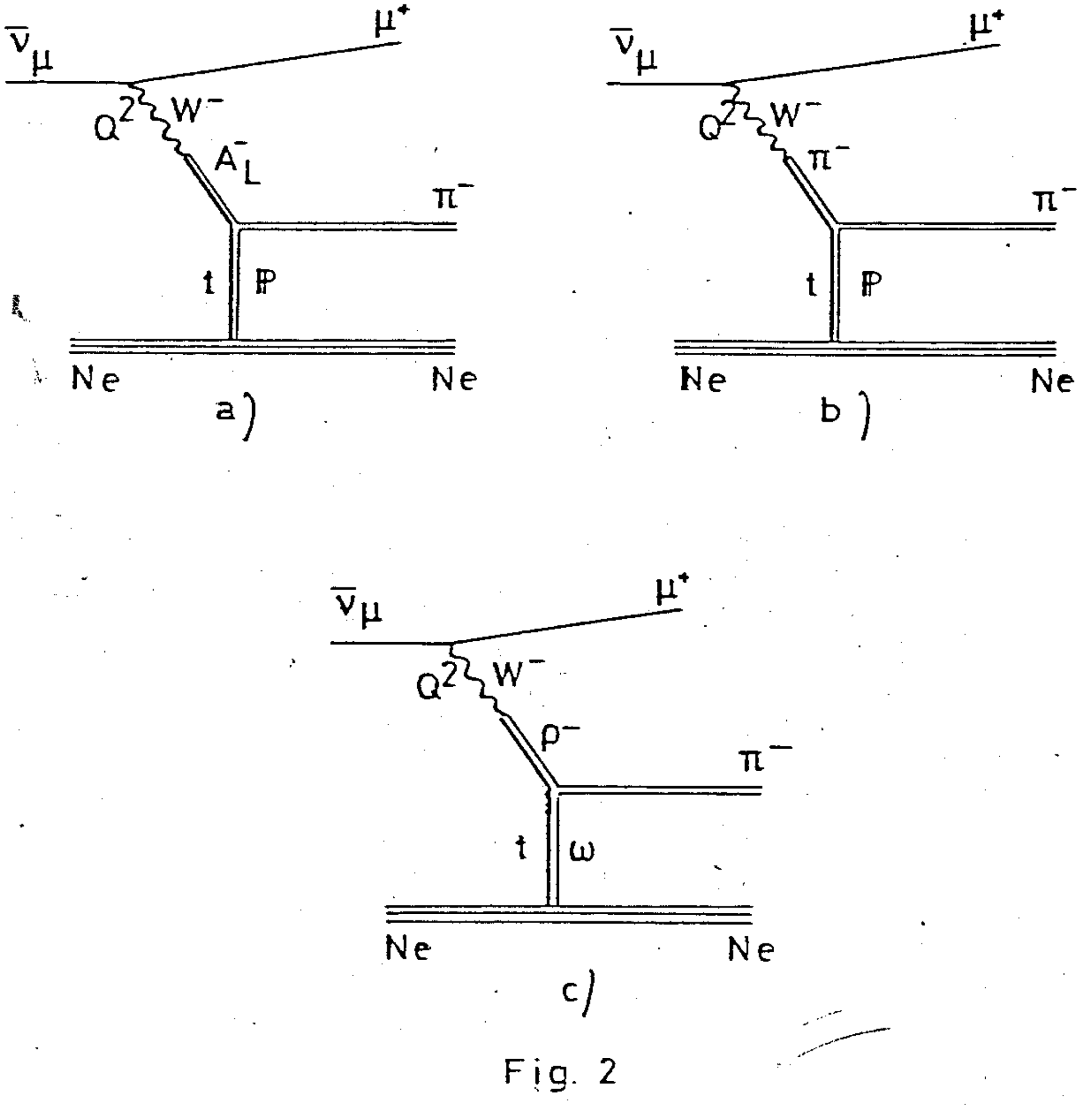
$\overline{\nu}_\mu$
μ^+
Q^2
W^-
A_L^-
π^-
t
ℙ
Ne
Ne
a)
$\overline{\nu}_\mu$
μ^+
Q^2
W^-
π^-
π^-
t
ℙ
Ne
Ne
b)
$\overline{\nu}_\mu$
μ^+
Q^2
W^-
ρ^-
π^-
t
ω
Ne
Ne
c)

Fig. 2

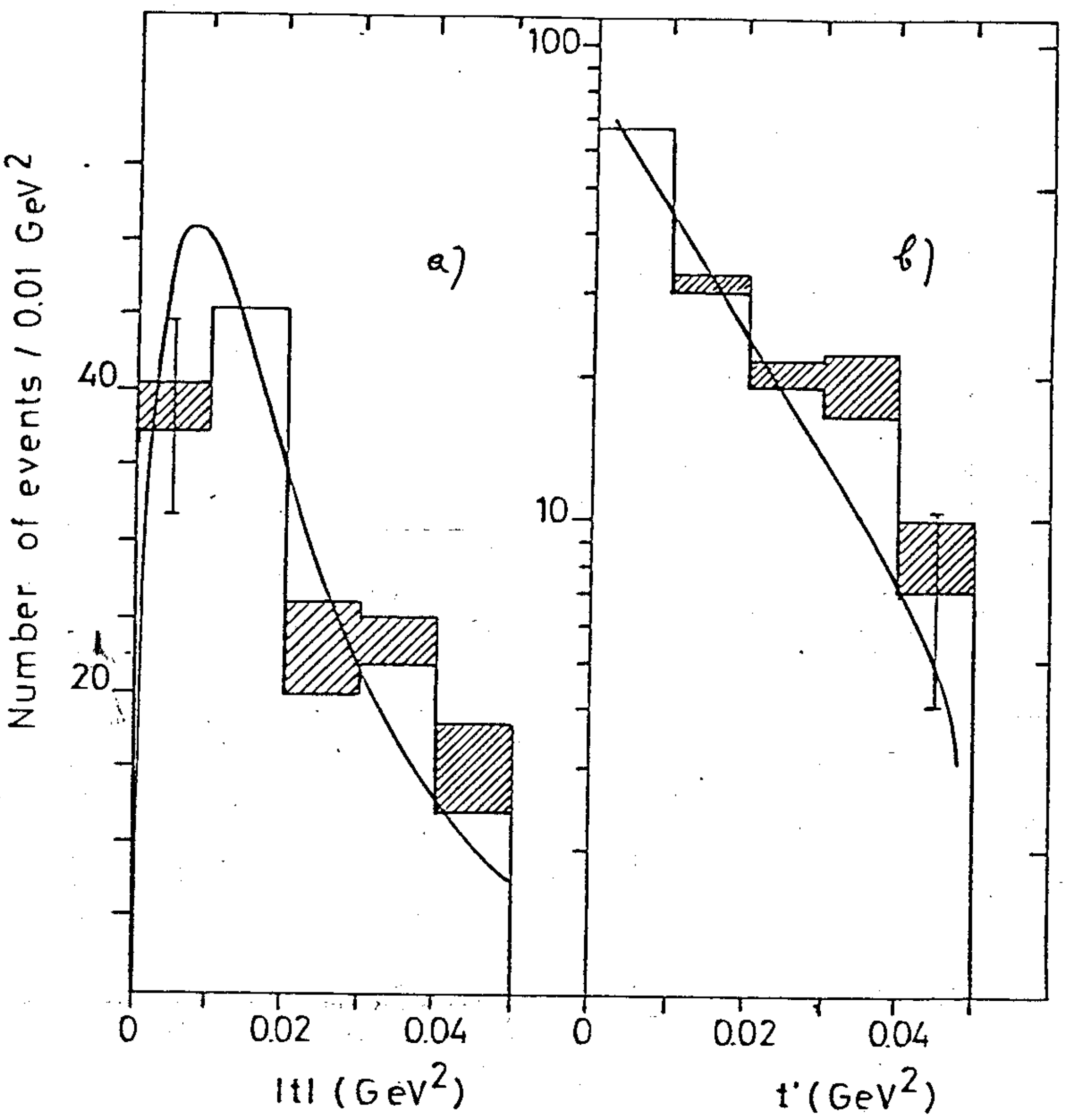

Number of events / 0.01 GeV 2
40
20
a)
0
0.02
0.04
|t| (GeV^2)
100
10
b)
0
0.02
0.04
t' (GeV^2)

Fig. 3

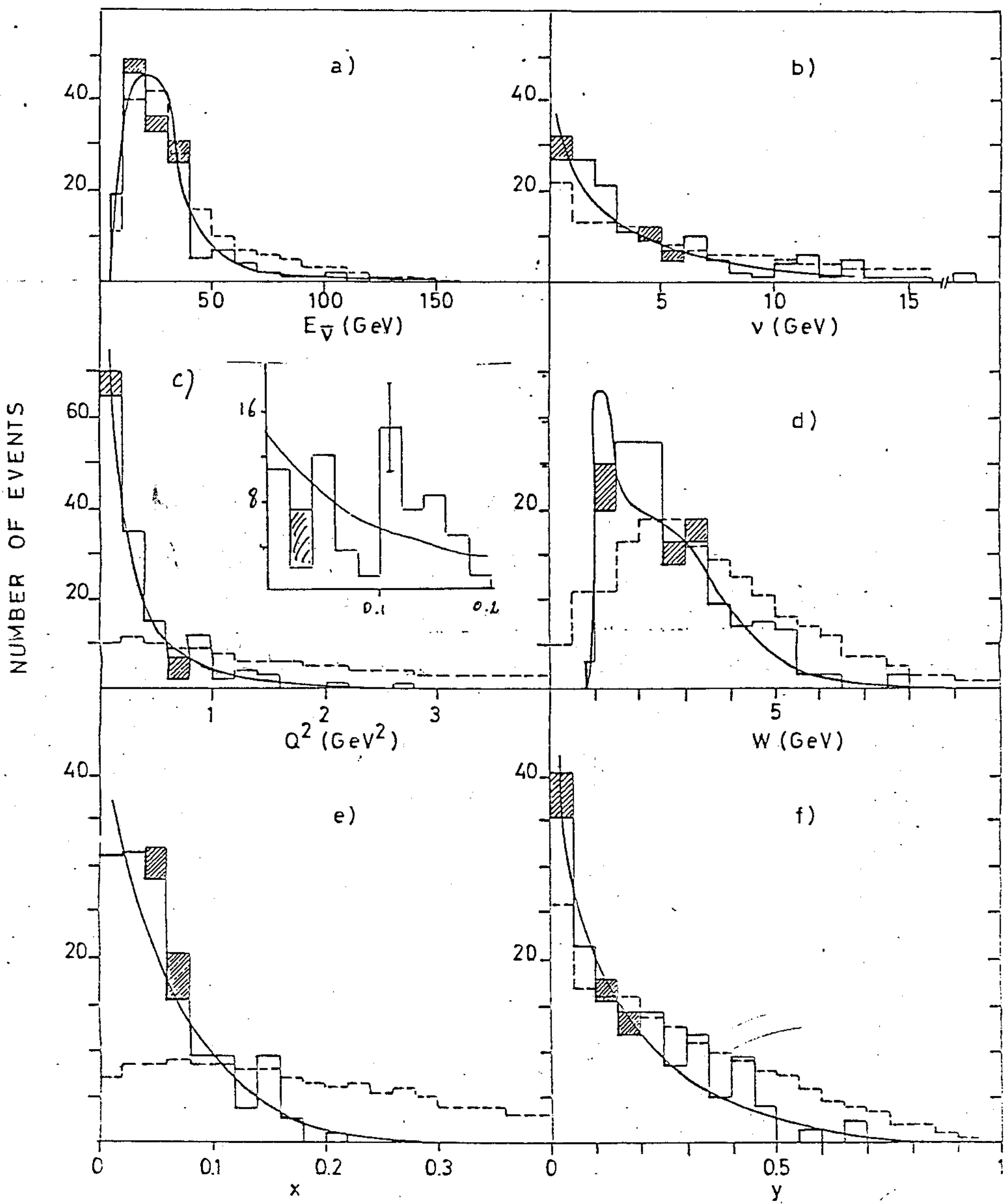
NUMBER OF EVENTS
a)
40
20
50
100
150
$E_{\bar{\nu}}$ (GeV)
b)
40
20
5
10
15
ν (GeV)
c)
60
40
20
1
2
3
Q^2 (GeV^2)
16
8
0.1
0.2
d)
20
5
W (GeV)
e)
40
20
0
0.1
0.2
0.3
x
f)
40
20
0
0.5
1
y

Fig. 4

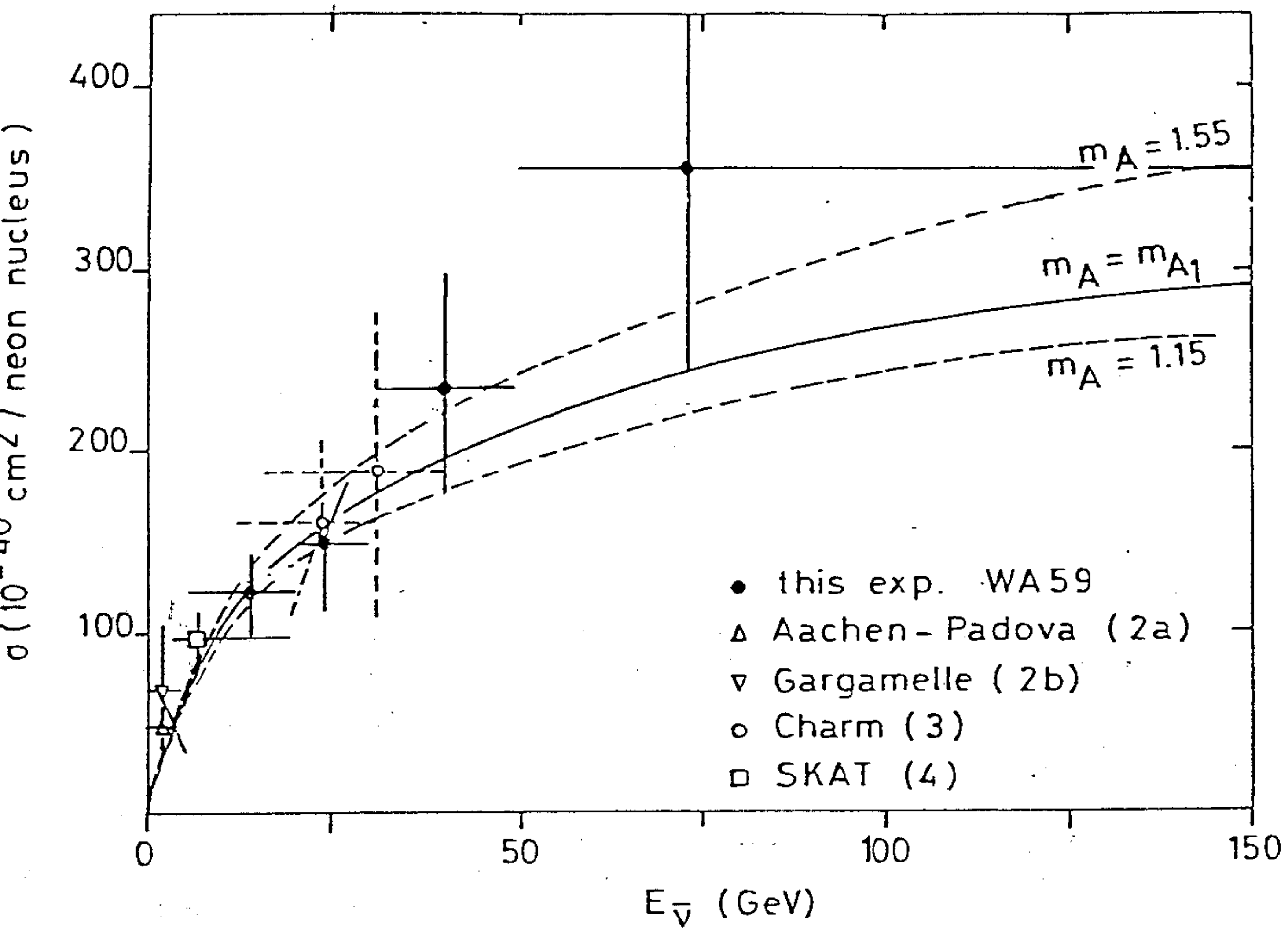

400
300
200
100
0
50
100
150
σ (10⁻⁴⁰ cm² / neon nucleus)
E$_{\bar{\nu}}$ (GeV)
m$_A$ = 1.55
m$_A$ = m$_{A1}$
m$_A$ = 1.15
● this exp. WA59
△ Aachen - Padova (2a)
▽ Gargamelle (2b)
○ Charm (3)
□ SKAT (4)

Fig. 5